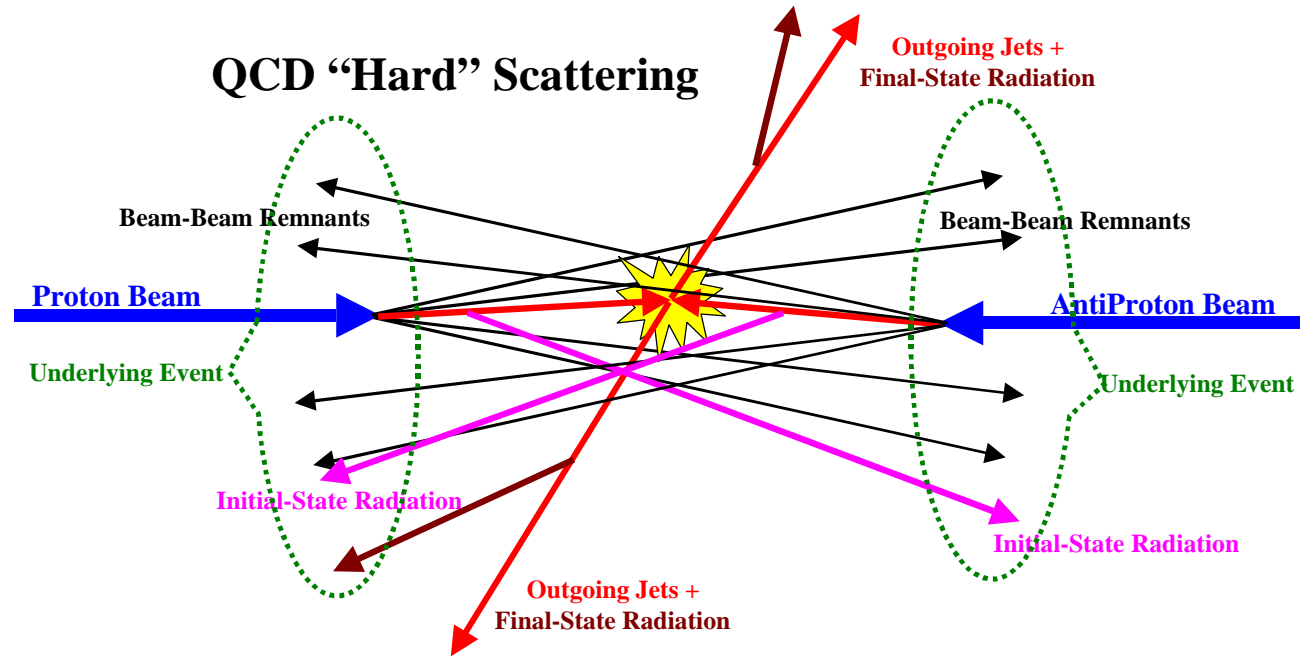


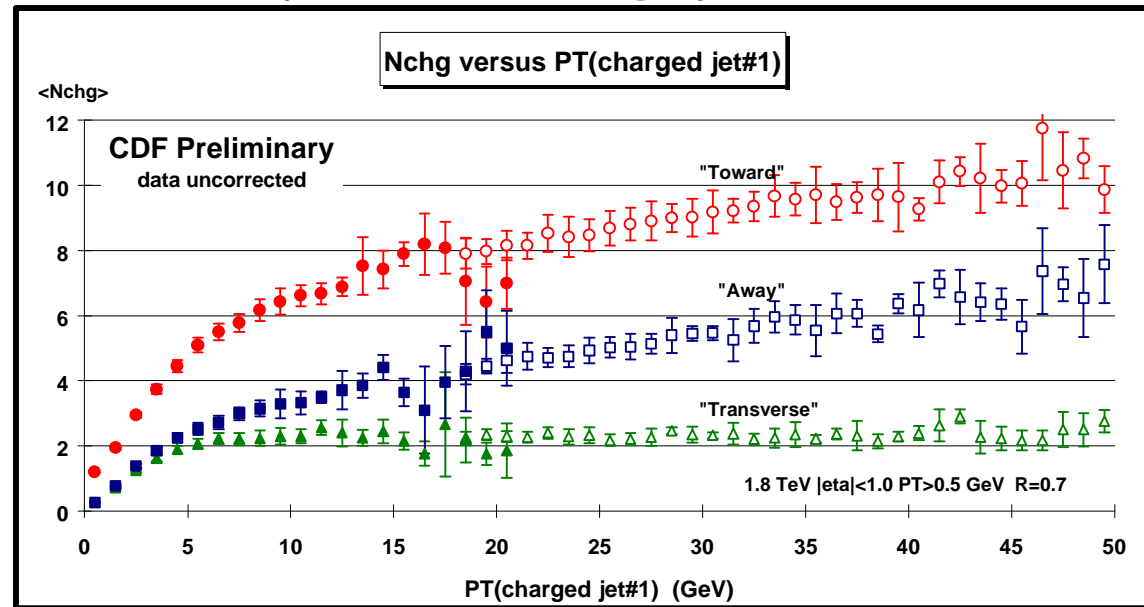
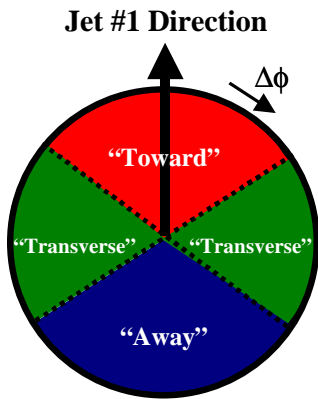
Min-Bias Physics: The Underlying Event



The “**Underlying Event**” consists of the **beam-beam remnants**, **initial-state radiation**, and sometimes **final-state radiation**.

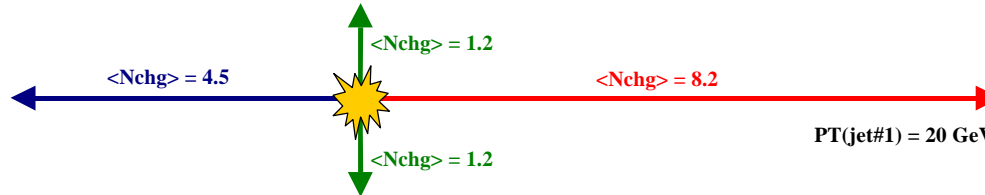
Min-Bias Physics: The Underlying Event

Blessed Plot 4: “Toward”, “Transverse”, “Away” $\langle N_{chg} \rangle$ vs $PT(\text{charged jet\#1})$:



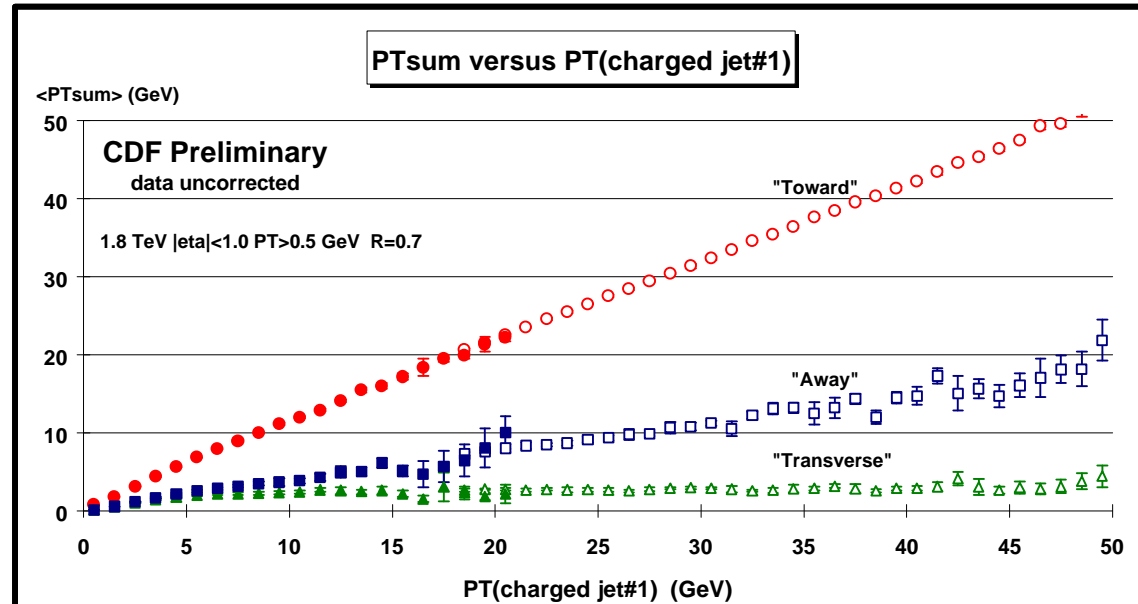
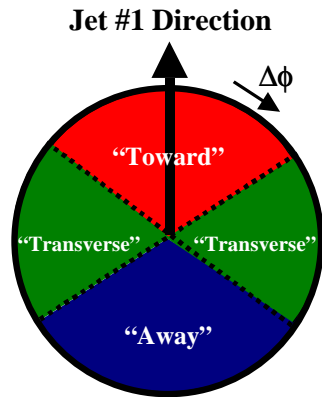
Plot shows the average number of toward ($|\phi| < 60^\circ$), transverse ($60 < |\phi| < 120^\circ$), and away ($|\phi| > 120^\circ$) charged particles ($PT > 0.5$ GeV, $|\eta| < 1$ including jet#1) as a function of the PT of the leading charged jet. The errors on the (uncorrected) data include both statistical and correlated systematic uncertainties.

Event Shape for $PT(\text{charged jet\#1}) = 20$ GeV (uncorrected):



Min-Bias Physics: The Underlying Event

Blessed Plot 5: “Toward”, “Transverse”, “Away” $\langle PT_{sum} \rangle$ vs $PT(\text{charged jet\#1})$:



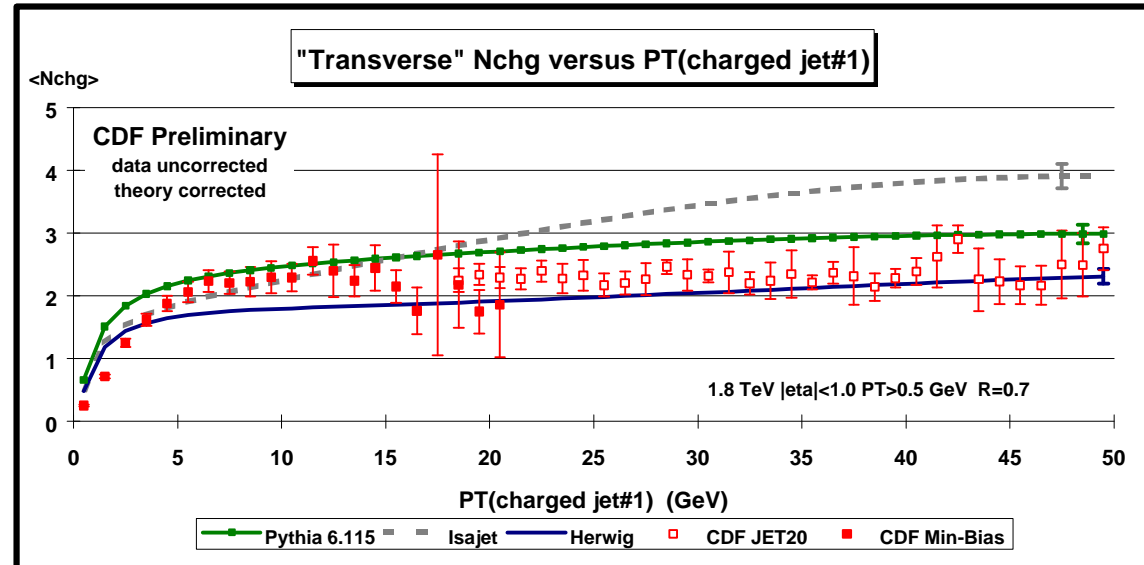
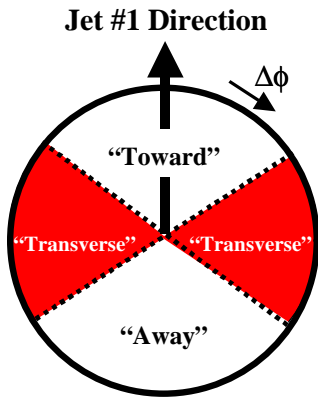
Plot shows the average PT_{sum} of toward ($|\phi| < 60^\circ$), transverse ($60 < |\phi| < 120^\circ$), and away ($|\phi| > 120^\circ$) charged particles ($PT > 0.5$ GeV, $|\eta| < 1$ including jet#1) as a function of the PT of the leading charged jet. The errors on the (uncorrected) data include both statistical and correlated systematic uncertainties.

Event Shape for $PT(\text{charged jet\#1}) = 20$ GeV (uncorrected):



Min-Bias Physics: The Underlying Event

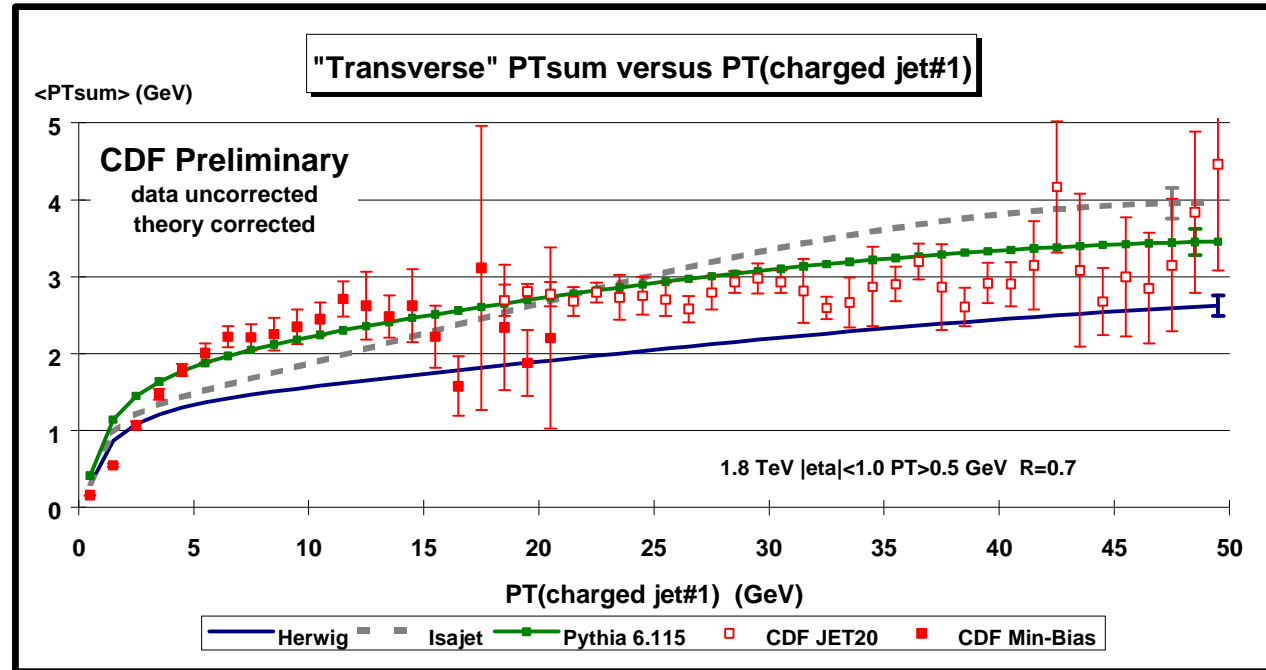
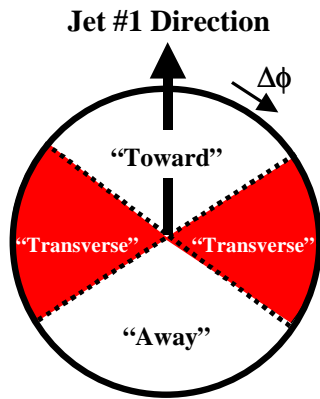
Blessed Plot 7: “Transverse” $\langle N_{chg} \rangle$ vs PT(charged jet#1):



Plot shows the average number of transverse ($60 < |\phi| < 120^\circ$) charged particles ($PT > 0.5$ GeV, $|\eta| < 1$ including jet#1) as a function of the PT of the leading charged jet. The errors on the (uncorrected) data include both statistical and correlated systematic uncertainties. The QCD “hard scattering” theory curves (Herwig 5.9, Isajet 7.32, Pythia 6.115) are corrected for the track finding efficiency and have an error (statistical plus systematic) of around 5%.

Min-Bias Physics: The Underlying Event

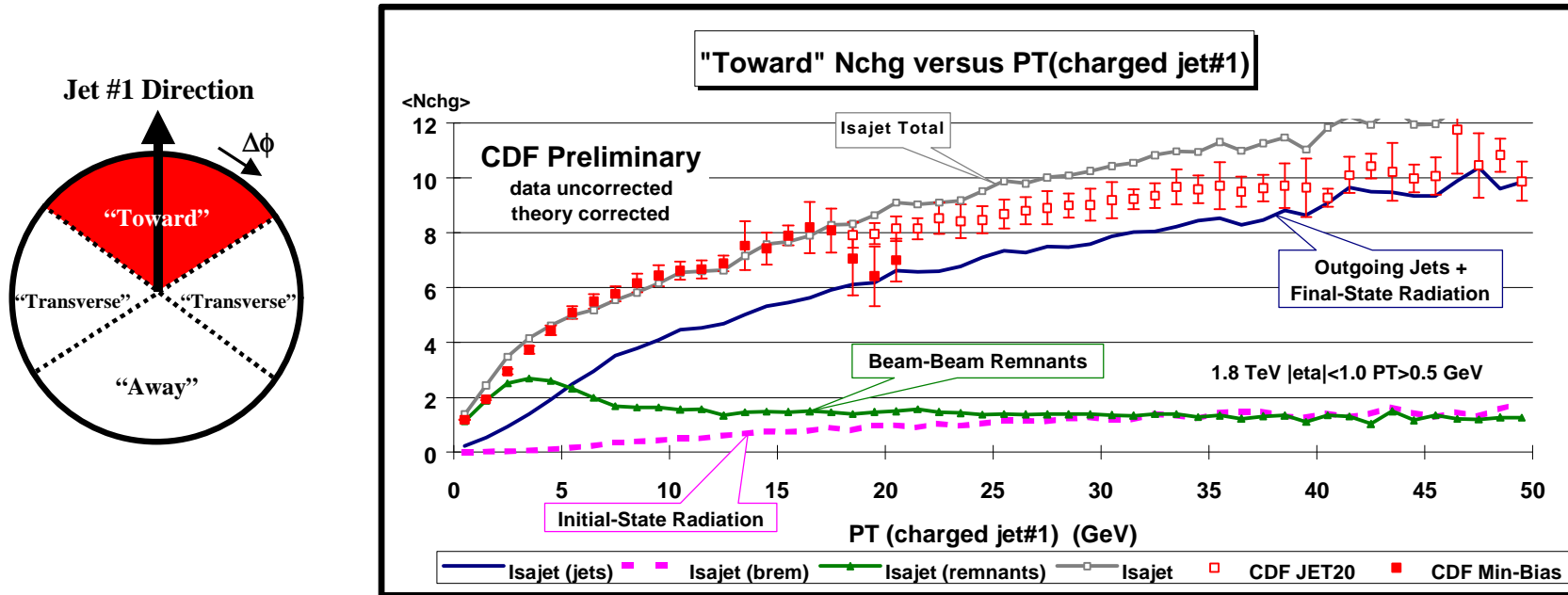
Blessed Plot 8: “Transverse” $\langle PT_{sum} \rangle$ vs $PT(\text{charged jet\#1})$:



Plot shows the average PT_{sum} of transverse ($60 < |\phi| < 120^\circ$) charged particles ($PT > 0.5$ GeV, $|\eta| < 1$ including Jet#1) as a function of the PT of the leading charged jet. The errors on the (uncorrected) data include both statistical and correlated systematic uncertainties. The QCD “hard scattering” theory curves (Herwig 5.9, Isajet 7.32, Pythia 6.115) are corrected for the track finding efficiency and have an error (statistical plus systematic) of around 5%.

Min-Bias Physics: The Underlying Event

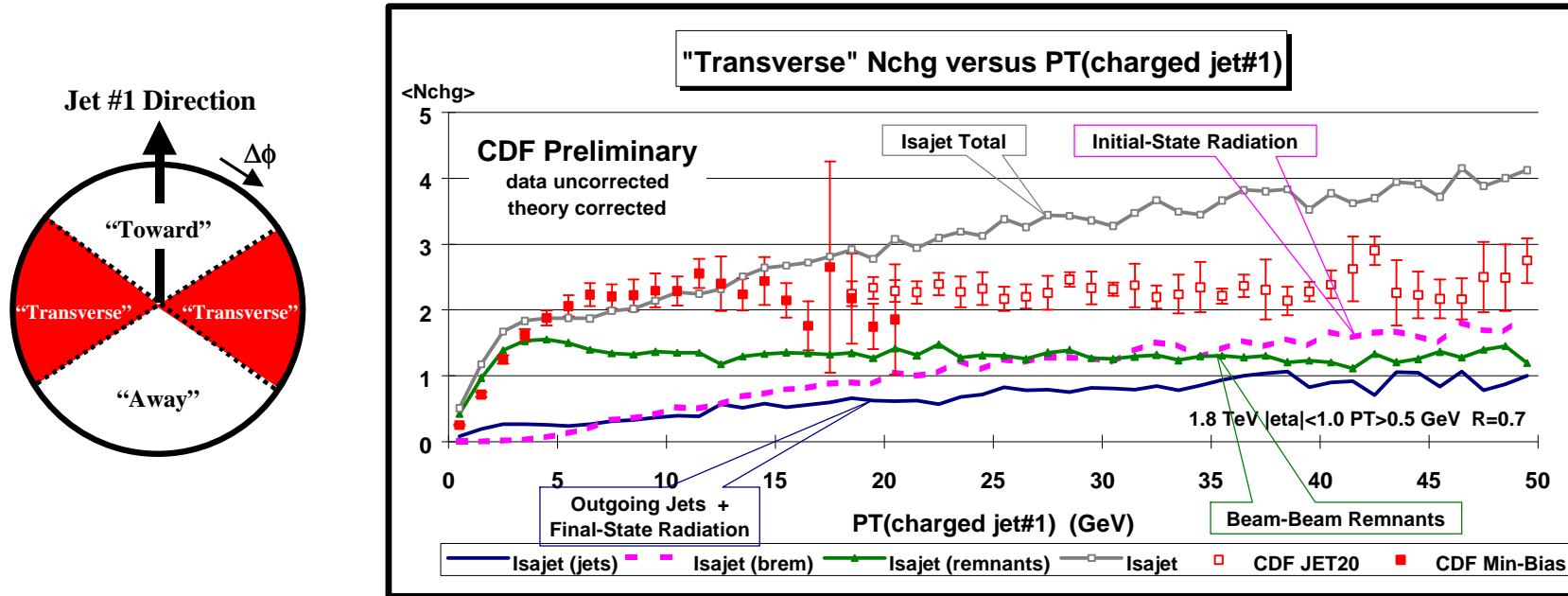
New Plot 1: “Toward” $\langle N_{chg} \rangle$ vs PT(charged jet#1) compared with Isajet:



Plot shows the average number of toward ($|\phi| < 60^\circ$) charged particles ($PT > 0.5$ GeV, $|\eta| < 1$, including jet#1) as a function of the PT of the leading charged jet. The errors on the (uncorrected) data include both statistical and correlated systematic uncertainties. The QCD “hard scattering” theory curves (Isajet 7.32) are corrected for the track finding efficiency and have an error (statistical plus systematic) of around 5%. The predictions of Isajet are divided into three categories: charged particles that arise from the break-up of the beam and target (beam-beam remnants), charged particles that arise from initial-state radiation (brem), and charged particles that result from the outgoing jets plus final-state radiation (jets).

Min-Bias Physics: The Underlying Event

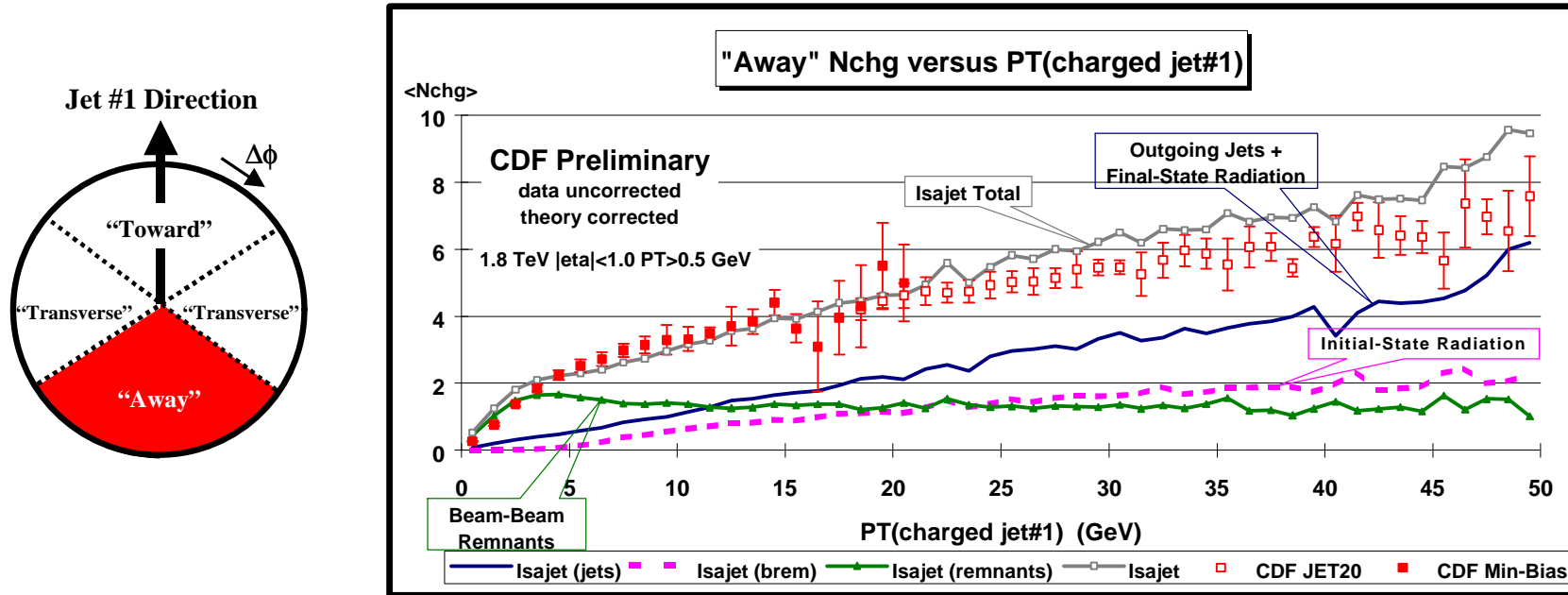
New Plot 2: “Transverse” $\langle N_{chg} \rangle$ vs PT(charged jet#1) compared with Isajet:



Plot shows the average number of transverse ($60 < |\phi| < 120^\circ$) charged particles ($PT > 0.5$ GeV, $|\eta| < 1$) as a function of the PT of the leading charged jet. The errors on the (uncorrected) data include both statistical and correlated systematic uncertainties. The QCD “hard scattering” theory curves (Isajet 7.32) are corrected for the track finding efficiency and have an error (statistical plus systematic) of around 5%. The predictions of Isajet are divided into three categories: charged particles that arise from the break-up of the beam and target (beam-beam remnants), charged particles that arise from initial-state radiation (brem), and charged particles that result from the outgoing jets plus final-state radiation (jets).

Min-Bias Physics: The Underlying Event

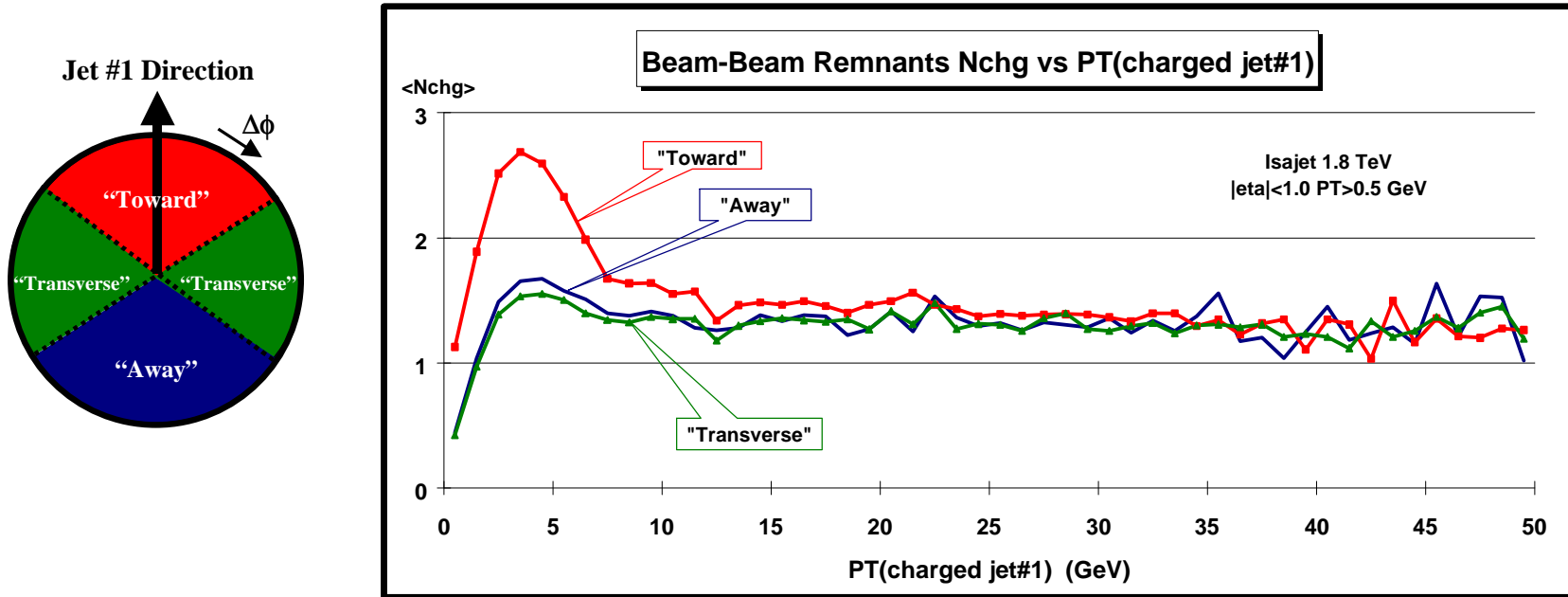
New Plot 3: “Away” $\langle N_{chg} \rangle$ vs $PT(\text{charged jet\#1})$ compared with **Isajet:**



Plot shows the average number of away ($|\phi| > 120^\circ$) charged particles ($PT > 0.5 \text{ GeV}$, $|\eta| < 1$) as a function of the PT of the leading charged jet. The errors on the (uncorrected) data include both statistical and correlated systematic uncertainties. The QCD “hard scattering” theory curves (Isajet 7.32) are corrected for the track finding efficiency and have an error (statistical plus systematic) of around 5%. The predictions of Isajet are divided into three categories: charged particles that arise from the break-up of the beam and target (beam-beam remnants), charged particles that arise from initial-state radiation (brem), and charged particles that result from the outgoing jets plus final-state radiation (jets).

Min-Bias Physics: The Underlying Event

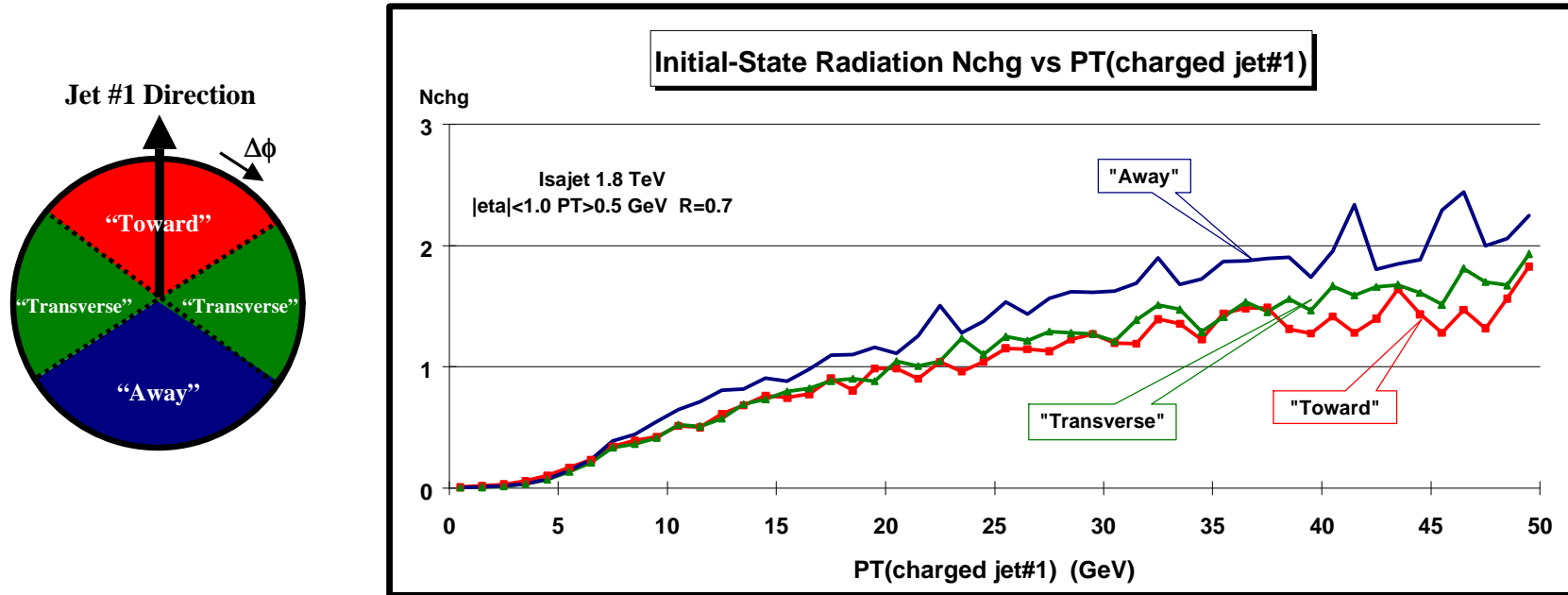
New Plot 4: Isajet “Toward”, “Transverse”, and “Away” $\langle N_{chg} \rangle$ vs $PT(\text{charged jet\#1})$:



Plot shows the average number of toward ($|\phi| < 60^\circ$), transverse ($60 < |\phi| < 120^\circ$), and away ($|\phi| > 120^\circ$) charged particles ($PT > 0.5$ GeV, $|\eta| < 1$ including jet#1) as a function of the PT of the leading charged jet from Isajet. The QCD “hard scattering” theory curves (Isajet 7.32) are corrected for the track finding efficiency and have an error (statistical plus systematic) of around 5%. The plot shows only those charged particles that arise from the break-up of the beam and target (beam-beam remnants).

Min-Bias Physics: The Underlying Event

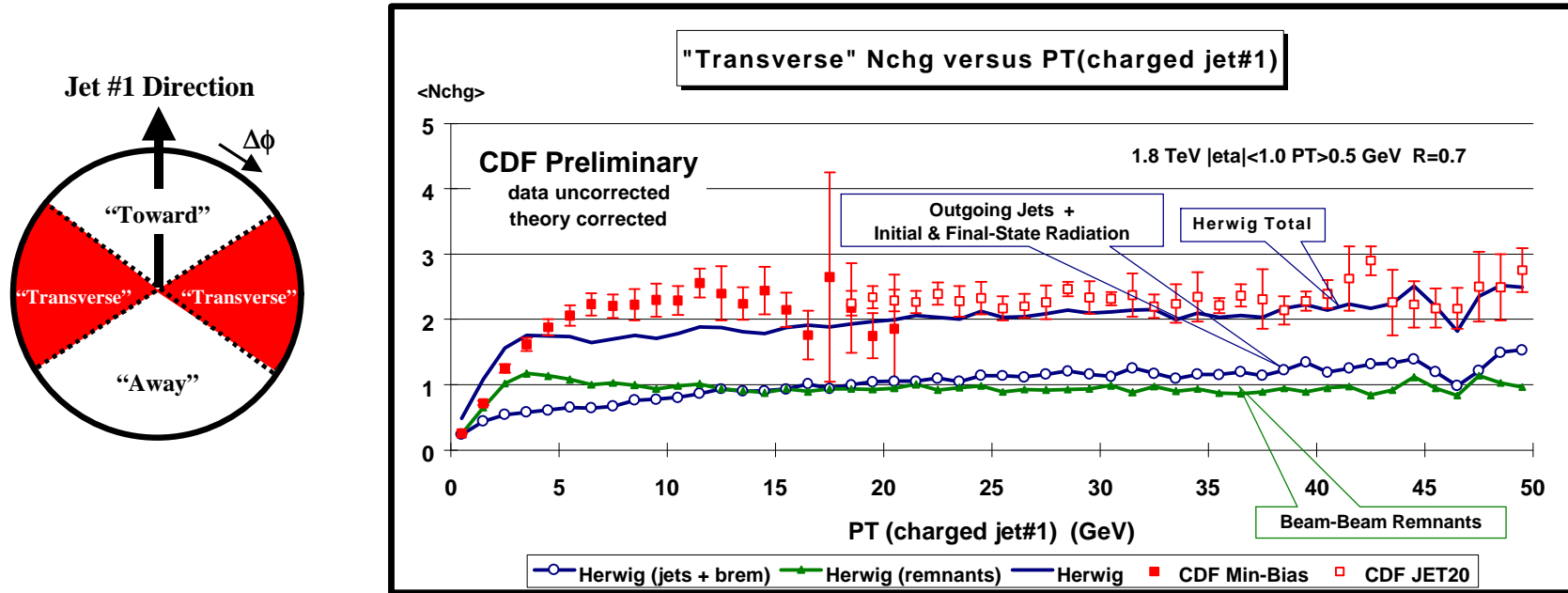
New Plot 5: Isajet “Toward”, “Transverse”, and “Away” $\langle N_{chg} \rangle$ vs PT(charged jet#1):



Plot shows the average number of toward ($|\phi| < 60^\circ$), transverse ($60 < |\phi| < 120^\circ$), and away ($|\phi| > 120^\circ$) charged particles ($PT > 0.5$ GeV, $|\eta| < 1$ including jet#1) as a function of the PT of the leading charged jet from Isajet. The QCD “hard scattering” theory curves (Isajet 7.32) are corrected for the track finding efficiency and have an error (statistical plus systematic) of around 5%. The plot shows only those charged particles that arise from initial-state radiation

Min-Bias Physics: The Underlying Event

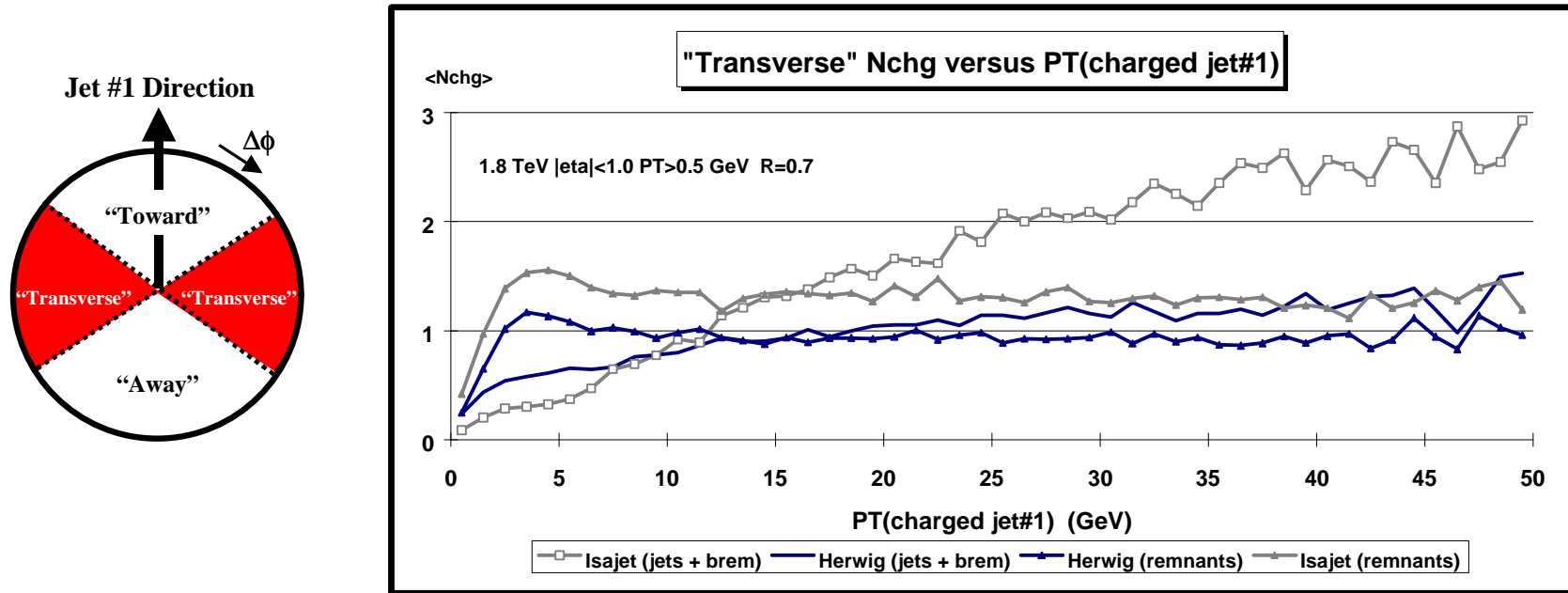
New Plot 6: “Transverse” $\langle N_{chg} \rangle$ vs PT(charged jet#1) compared with Herwig:



Plot shows the average number of transverse ($60 < |\phi| < 120^\circ$) charged particles ($PT > 0.5 \text{ GeV}$, $|\eta| < 1$) as a function of the PT of the leading charged jet. The errors on the (uncorrected) data include both statistical and correlated systematic uncertainties. The QCD “hard scattering” theory curves (Herwig 5.9) are corrected for the track finding efficiency and have an error (statistical plus systematic) of around 5%. The predictions of Herwig are divided into two categories: charged particles that arise from the break-up of the beam and target (beam-beam remnants), and charged particles that result from the outgoing jets plus initial and final-state radiation (jets + brem).

Min-Bias Physics: The Underlying Event

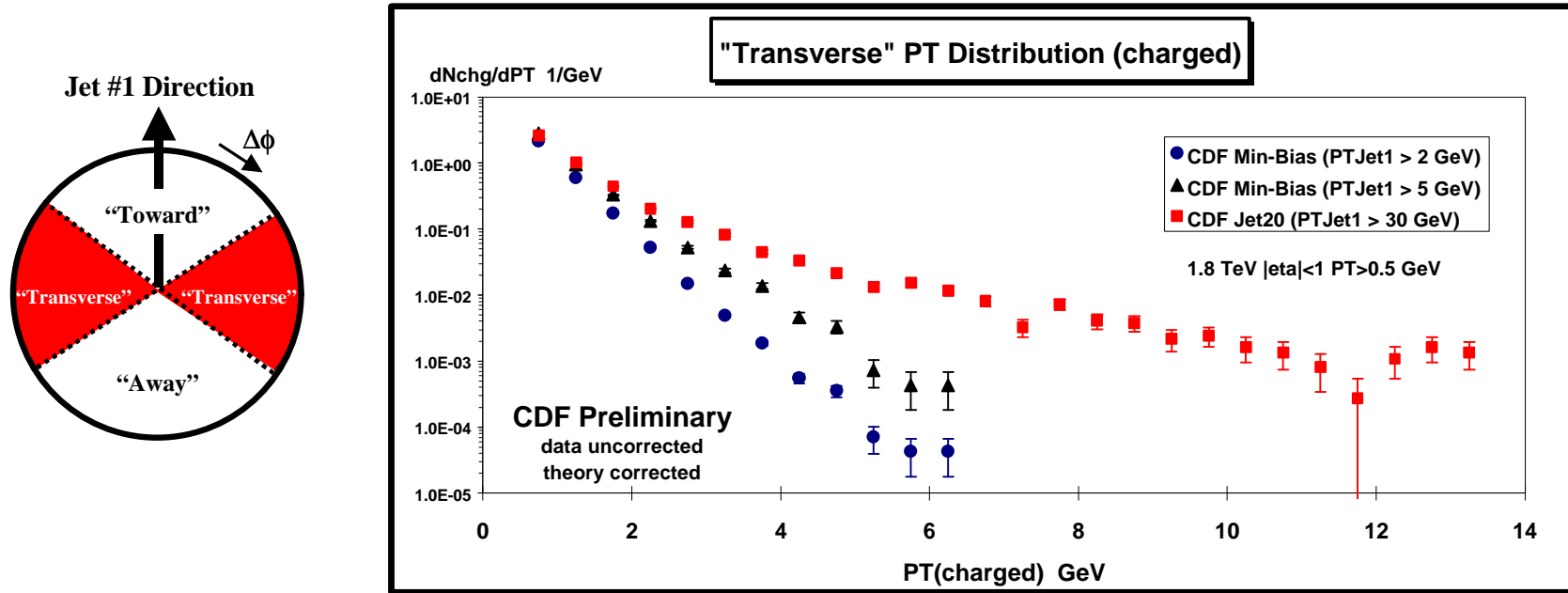
New Plot 7: Isajet and Herwig “Transverse” $\langle N_{chg} \rangle$ vs $PT(\text{charged jet\#1})$:



Plot shows the average number of transverse ($60 < \phi < 120^\circ$) charged particles ($PT > 0.5 \text{ GeV}$, $|\eta| < 1$) as a function of the PT of the leading charged jet. The QCD “hard scattering” theory curves (Isajet 7.32, Herwig 5.9) are corrected for the track finding efficiency and have an error (statistical plus systematic) of around 5%. The predictions of Isajet and Herwig are divided into two categories: charged particles that arise from the break-up of the beam and target (beam-beam remnants), and charged particles that result from the outgoing jets plus initial and final-state radiation (jets + brem).

Min-Bias Physics: The Underlying Event

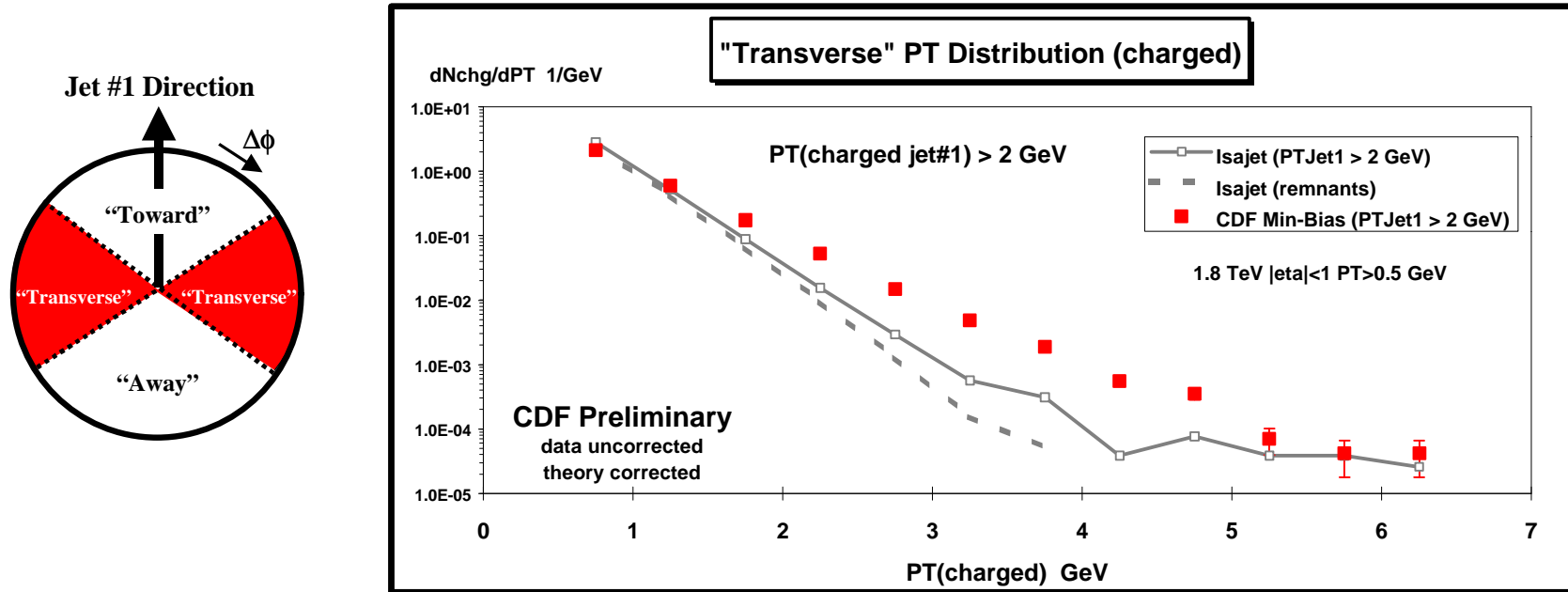
New Plot 8: “Transverse” PT Distribution for PT(charged jet#1) > 2, 5, and 30 GeV:



Plot shows the PT distribution of transverse ($60 < |\phi| < 120^\circ$) charged particles ($PT > 0.5 \text{ GeV}$, $|\eta| < 1$) for $PT(\text{charged jet\#1}) > 2, 5, \text{ and } 30 \text{ GeV}$. The points correspond to dN_{chg}/dPT (the integral is the average number of transverse charged particles). The errors on the (uncorrected) data are statistical only.

Min-Bias Physics: The Underlying Event

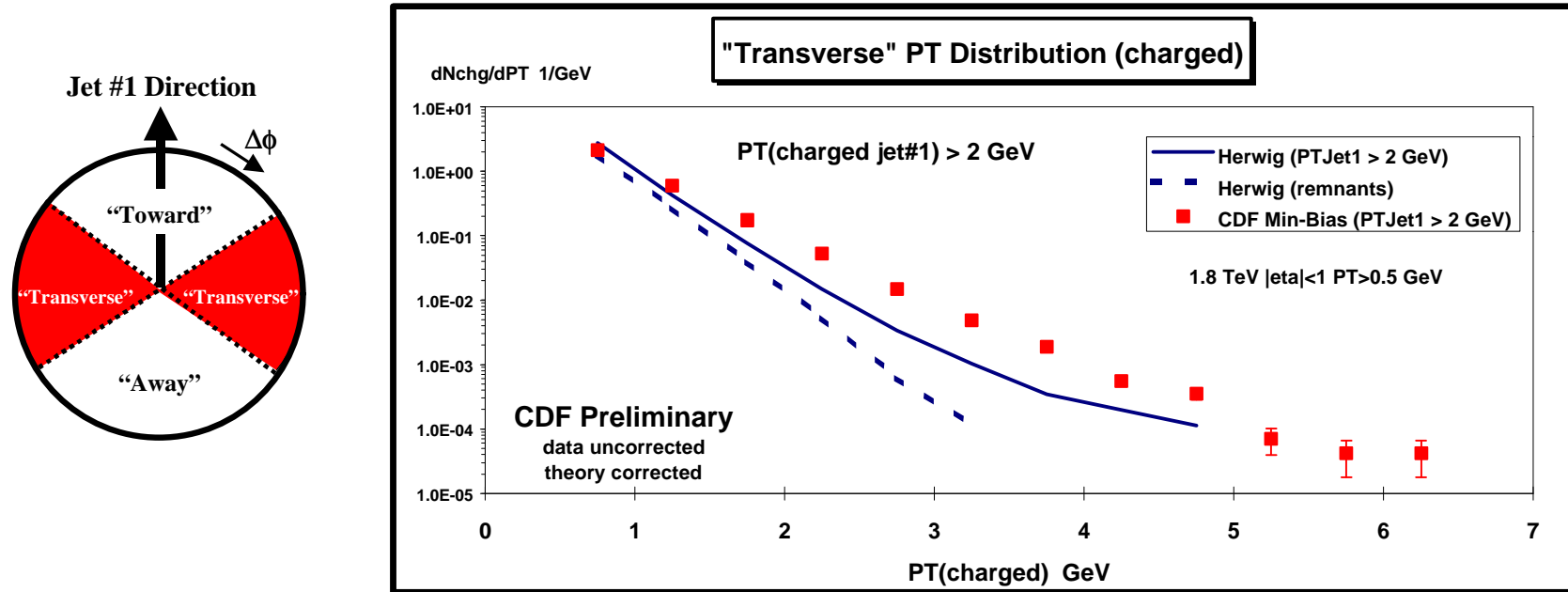
New Plot 9: “Transverse” PT Distribution for PT(charged jet#1) > 2 GeV compared with Isajet:



Plot shows the PT distribution of transverse ($60 < |\phi| < 120^\circ$) charged particles ($PT > 0.5 \text{ GeV}$, $|\eta| < 1$) for $PT(\text{charged jet\#1}) > 2 \text{ GeV}$. The points correspond to dN_{chg}/dPT (the integral is the average number of transverse charged particles). The errors on the (uncorrected) data are statistical only. The QCD “hard scattering” theory curves (Isajet 7.32) are corrected for the track finding efficiency. The predictions of Isajet are divided into two categories: charged particles that arise from the break-up of the beam and target (beam-beam remnants), and charged particles that result from the outgoing jets plus initial and final-state radiation (jets + brem). The solid (dashed) curve corresponds to the total (beam-beam remnants).

Min-Bias Physics: The Underlying Event

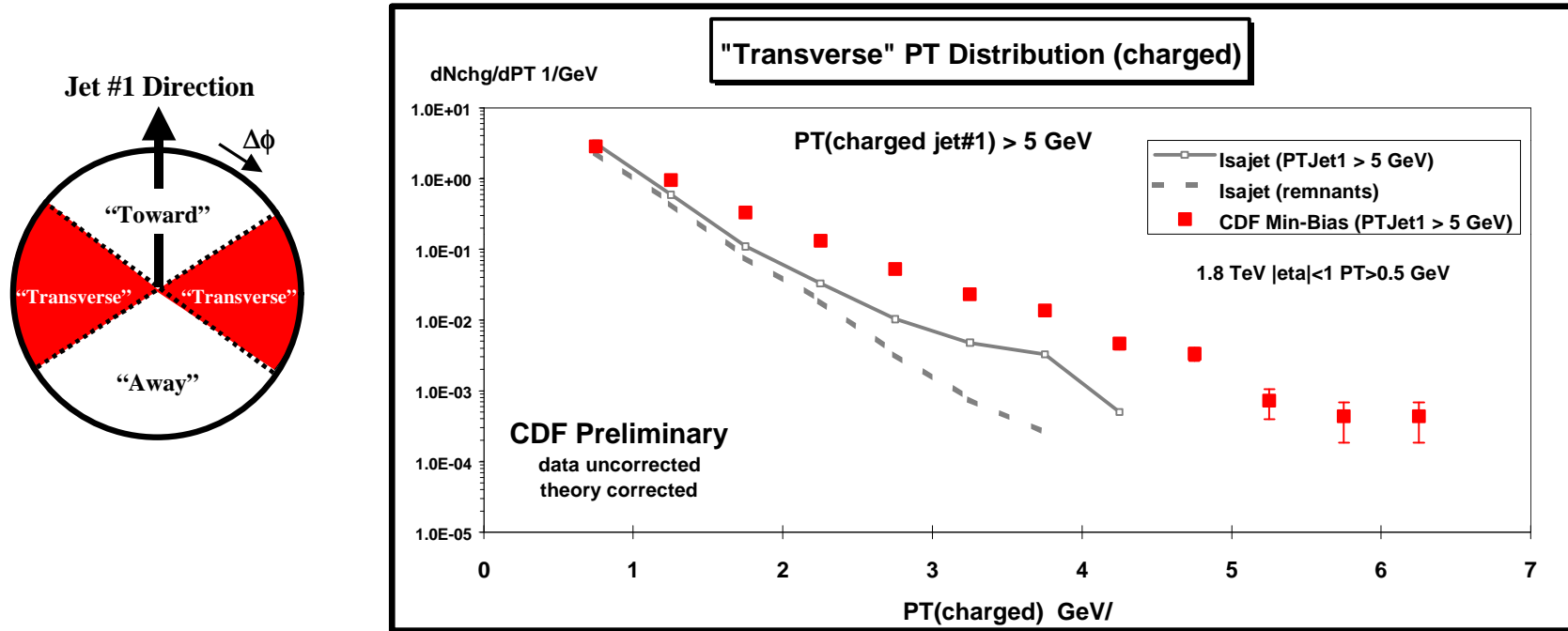
New Plot 10: “Transverse” PT Distribution for $PT(\text{charged jet\#1}) > 2 \text{ GeV}$ compared with Herwig:



Plot shows the PT distribution of transverse ($60 < |\phi| < 120^\circ$) charged particles ($PT > 0.5 \text{ GeV}$, $|\eta| < 1$) for $PT(\text{charged jet\#1}) > 2 \text{ GeV}$. The points correspond to dN_{chg}/dPT (the integral is the average number of transverse charged particles). The errors on the (uncorrected) data are statistical only. The QCD “hard scattering” theory curves (Herwig 5.9) are corrected for the track finding efficiency. The predictions of Herwig are divided into two categories: charged particles that arise from the break-up of the beam and target (beam-beam remnants), and charged particles that result from the outgoing jets plus initial and final-state radiation (jets + brem). The solid (dashed) curve corresponds to the total (beam-beam remnants).

Min-Bias Physics: The Underlying Event

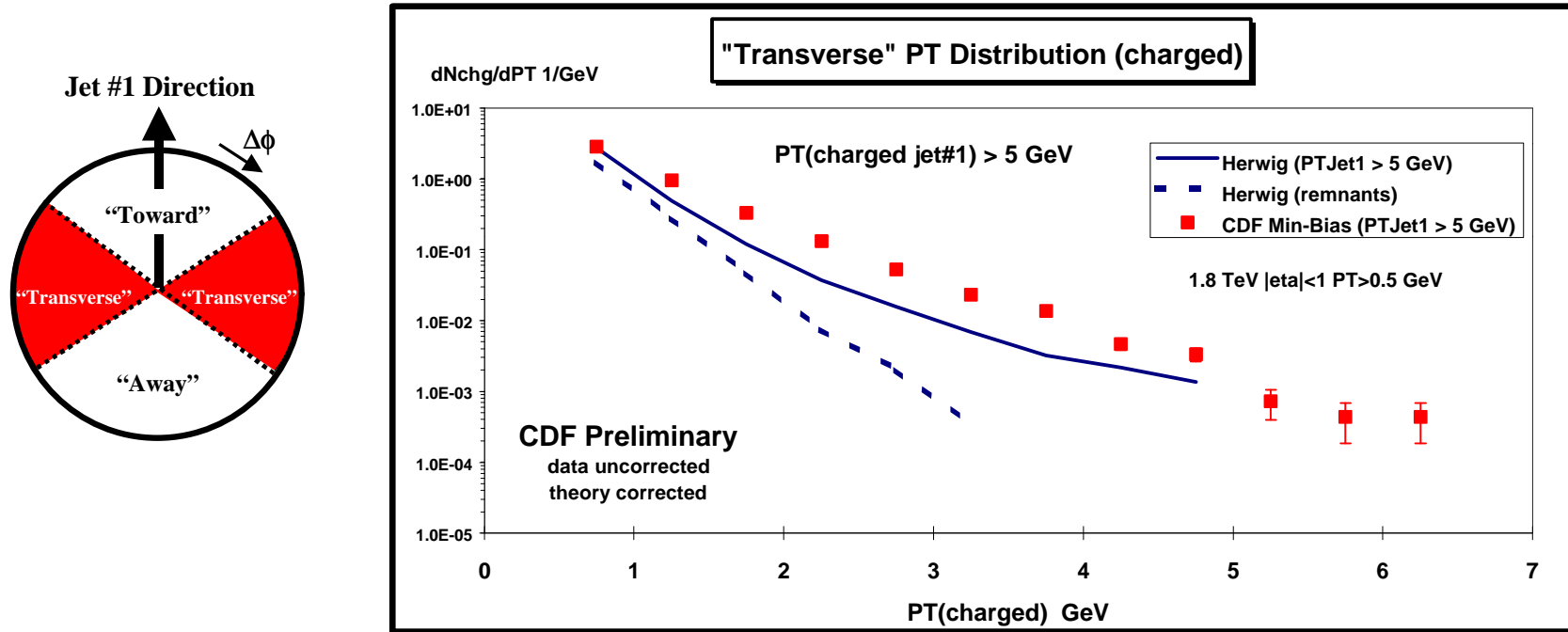
New Plot 11: “Transverse” PT Distribution for PT(charged jet#1) > 5 GeV compared with Isajet:



Plot shows the PT distribution of transverse ($60 < |\phi| < 120^\circ$) charged particles ($PT > 0.5 \text{ GeV}$, $|\eta| < 1$) for $PT(\text{charged jet\#1}) > 5 \text{ GeV}$. The points correspond to dN_{chg}/dPT (the integral is the average number of transverse charged particles). The errors on the (uncorrected) data are statistical only. The QCD “hard scattering” theory curves (Isajet 7.32) are corrected for the track finding efficiency. The predictions of Isajet are divided into two categories: charged particles that arise from the break-up of the beam and target (beam-beam remnants), and charged particles that result from the outgoing jets plus initial and final-state radiation (jets + brem). The solid (dashed) curve corresponds to the total (beam-beam remnants).

Min-Bias Physics: The Underlying Event

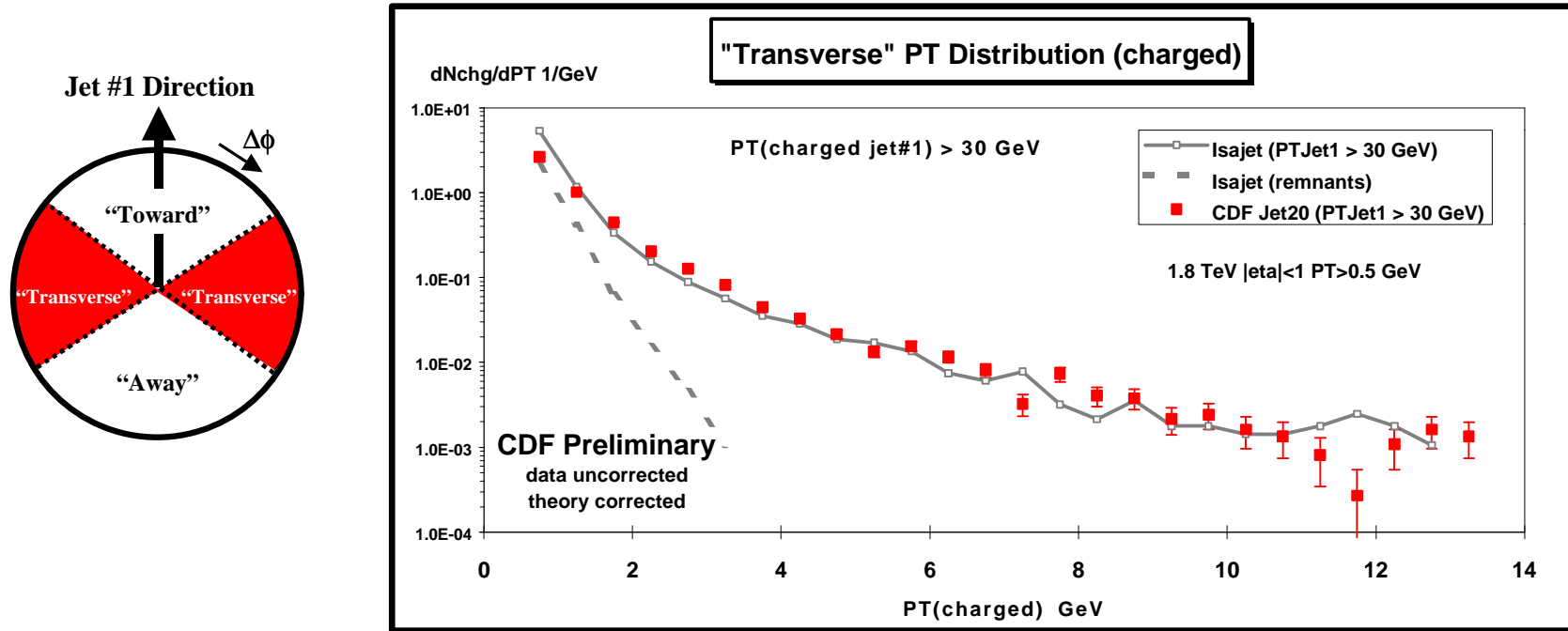
New Plot 12: “Transverse” PT Distribution for $PT(\text{charged jet}\#1) > 5 \text{ GeV}$ compared with Herwig:



Plot shows the PT distribution of transverse ($60 < |\phi| < 120^\circ$) charged particles ($PT > 0.5 \text{ GeV}$, $|\eta| < 1$) for $PT(\text{charged jet}\#1) > 5 \text{ GeV}$. The points correspond to dN_{chg}/dPT (the integral is the average number of transverse charged particles). The errors on the (uncorrected) data are statistical only. The QCD “hard scattering” theory curves (Herwig 5.9) are corrected for the track finding efficiency. The predictions of Herwig are divided into two categories: charged particles that arise from the break-up of the beam and target (beam-beam remnants), and charged particles that result from the outgoing jets plus initial and final-state radiation (jets + brem). The solid (dashed) curve corresponds to the total (beam-beam remnants).

Min-Bias Physics: The Underlying Event

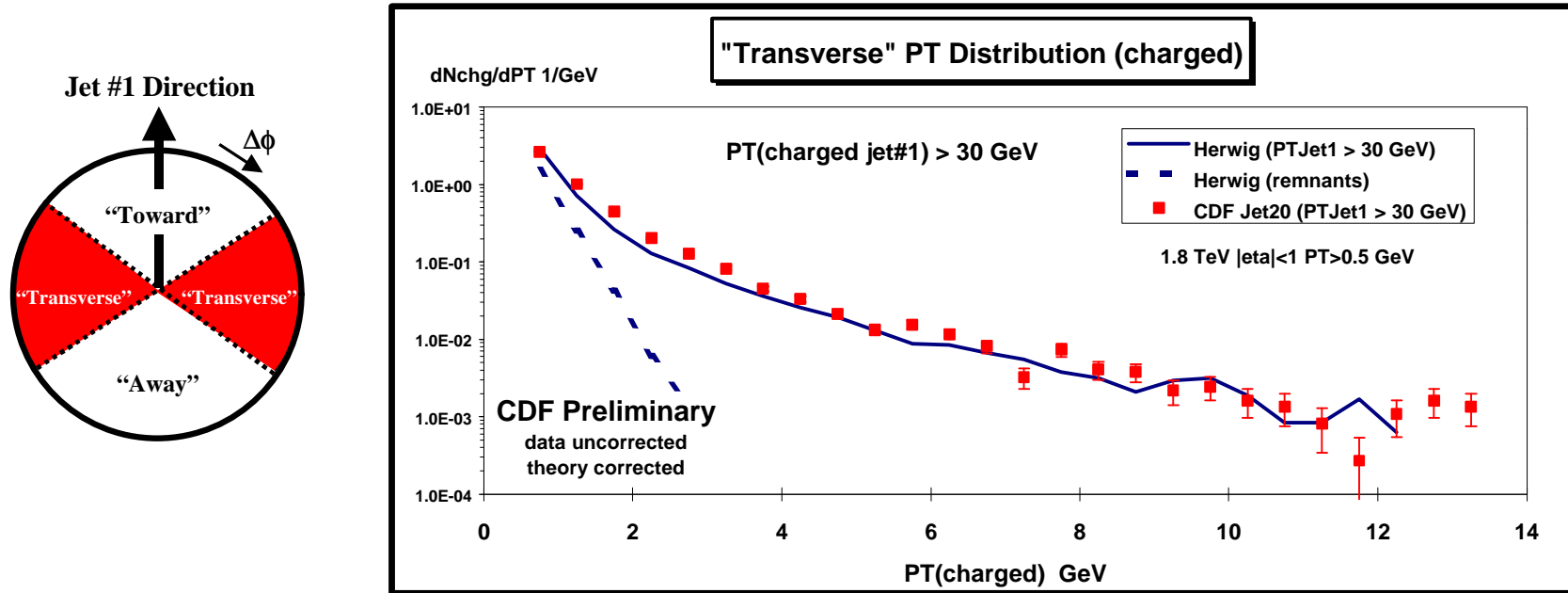
New Plot 13: “Transverse” PT Distribution for PT(charged jet#1) > 30 GeV compared with Isajet:



Plot shows the PT distribution of transverse ($60 < |\phi| < 120^\circ$) charged particles ($PT > 0.5 \text{ GeV}$, $|\eta| < 1$) for $PT(\text{charged jet\#1}) > 30 \text{ GeV}$. The points correspond to dN_{chg}/dPT (the integral is the average number of transverse charged particles). The errors on the (uncorrected) data are statistical only. The QCD “hard scattering” theory curves (Isajet 7.32) are corrected for the track finding efficiency. The predictions of Isajet are divided into two categories: charged particles that arise from the break-up of the beam and target (beam-beam remnants), and charged particles that result from the outgoing jets plus initial and final-state radiation (jets + brem). The solid (dashed) curve corresponds to the total (beam-beam remnants).

Min-Bias Physics: The Underlying Event

New Plot 14: “Transverse” PT Distribution for PT(charged jet#1) > 30 GeV compared with Herwig:



Plot shows the PT distribution of transverse ($60 < |\phi| < 120^\circ$) charged particles ($PT > 0.5 \text{ GeV}$, $|\eta| < 1$) for $PT(\text{charged jet\#1}) > 30 \text{ GeV}$. The points correspond to dN_{chg}/dPT (the integral is the average number of transverse charged particles). The errors on the (uncorrected) data are statistical only. The QCD “hard scattering” theory curves (Herwig 5.9) are corrected for the track finding efficiency. The predictions of Herwig are divided into two categories: charged particles that arise from the break-up of the beam and target (beam-beam remnants), and charged particles that result from the outgoing jets plus initial and final-state radiation (jets + brem). The solid (dashed) curve corresponds to the total (beam-beam remnants).